processes

MDPI

Review

A systems and treatment perspective of models of influenza virus-induced host responses

Ericka Mochan [1,2], Emily Ackerman [2] and Jason E. Shoemaker [2,3,4,*]

[1] Department of Mathematics, Carlow University, Pittsburgh PA 15213, USA
[2] Department of Chemical & Petroleum Engineering, University of Pittsburgh, Pittsburgh PA 15213, USA
[3] Department of Computational and Systems Biology, University of Pittsburgh, Pittsburgh PA 15213, USA
[4] McGowan Institute, University of Pittsburgh, Pittsburgh PA 15213, USA
* Correspondence: jason.shoemaker@pitt.edu

Received: date; Accepted: date; Published: date

Abstract: Severe influenza infections are often characterized as having unique host responses (e.g. early, severe hypercytokinemia). Neuraminidase inhibitors can be effective in controlling the severe symptoms of influenza but are often not administered until late in the infection. Several studies suggest that interferon pre-treatment may offer protection to high risk groups. We test three published ordinary differential equation models of the intrahost immune response during influenza infection to determine which facets of the immune response are most responsible for controlling virus titers over the course of the simulated infection. Each model emphasizes the importance of controlling the infected cell population in order to control viral replication. We also test each model's response to a pre-treatment of interferon before the virus is administered. Our work shows that the structure of current models does not allow for significant response to increased interferon. These results suggest that the current library of available published models of influenza infection does not adequately represent the complex interactions of the virus, interferon, and other aspects of the immune response. Specifically, the method used to model virus-resistant cells may need to be adapted in future work to more realistically represent the immune response to viral infection.

Keywords: mathematical modeling; influenza A virus; interferon pre-treatment; sensitivity analysis; systems biology

1. Introduction

Influenza A virus (IAV) leads to acute respiratory disease and significant morbidity and mortality around the world each year; the World Health Organization estimates 3 to 5 million cases of severe illness and 300,000-650,000 deaths worldwide every year are caused by IAV [1]. Generally, severe outcomes are limited to high-risk patient groups, i.e. infants, aged adults, or individuals with compromised immune systems. Occasionally, however, new strains emerge with pandemic potential which can induce severe disease across a broad portion of the population. For example, the 1918 Spanish influenza pandemic is estimated to have been responsible for the death of 2% of the world's population between 1918 and 1920 [2]. Several pandemics have occurred since, including outbreaks in 1957, 1968, and 2009 [3,4]. Experts believe that avian H5N1 influenza viruses pose the greatest risk to public health. H5N1 infections have demonstrated the ability to cause severe disease in humans, including symptoms such as fever, respiratory symptoms, lymphopenia, and cytokine storm (hypercytokinemia) [5–7]. Cytokine storm occurs when the host experiences out-of-control pro-inflammatory responses and insufficient anti-inflammatory responses to infection. This is often a result of severe influenza infection and causes acute respiratory distress syndrome (ARDS) and multiple organ failure in many patients [7].

Often, IAV infections are treated with neuraminidase inhibitors, such as oseltamivir (i.e. TamiFlu), which can be highly effective if administered during the early infection phase. However, IAV-infected hosts often do not seek treatment until late in their infection when the virus is already present at high levels and it may be too late for an effective treatment. Especially in the case of H5N1, neuraminidase inhibitors are often ineffective at containing cytokine storm and do not prevent the excess morbidity and mortality seen in these infections [8,9]. Moreover, oseltamivir-resistant strains can quickly evolve, as observed during the 2009 H1N1 pandemic [8].

1.1 Interferon pre-treatment and corticosteroid post-infection treatment of IAV infection

Corticosteroids have been suggested as a potential treatment option for patients undergoing severe IAV infection with accompanied cytokine storm, while interferon (IFN) treatment has been suggested to protect high-risk groups [7,10,11]. Corticosteroids have anti-inflammatory effects on the host and thus may be used to treat hypercytokinemia. The impact of corticosteroids on IAV-infected hosts is currently inconclusive. While some studies indicate steroids are effective in alleviating influenza symptoms in human patients [12], others have shown increased mortality in patients treated with corticosteroids [13]. IFN is a key regulator of the innate immune system, and pre-stimulation of IFN-regulating pathways has provided a preventative advantage in mice [11]. While promising as a protective agent for high-risk groups during a pandemic, little is known about the impact of pre-stimulation on hypercytokinemia.

Because of these contradictory results in human patients, there are no clear guidelines for steroid treatment of IAV-infected patients or or IFN pretreatment of high-risk groups. A previous study [14] showed that high dosages of triamcinolone were successful in suppressing inflammation in cotton rats infected with IAV, implying that a high steroid concentration is necessary for corticosteroids to be effective in controlling cytokine storm. Ultimately, effective treatment must be optimized to promote viral clearance while limiting inflammation and tissue degradation from hypercytokinemia.

1.2 Mathematical models of the lung host response to IAV infection

Mathematical models of the immune response in IAV-infected lungs have previously been used as a computational platform for treatment optimization [15–21]. In this work, we evaluate the ability of published mathematical models to simulate the administration of IFN treatment in hosts infected with IAV through a sensitivity analysis and the identification of highly sensitive components within each model. We find that virus concentration is largely influenced by the proportion of cells in the model that are able to become infected or virus-resistant; therefore, controlling these populations is paramount to controlling viral replication.

We analyzed three published models of the immune response to IAV: Saenz et al. 2010 [16], Pawelek et al. 2012 [15], and Hancioglu et al. 2007 [17]. Figure 1 depicts the interactions represented within each of the models. The Saenz and Pawelek models are trained to experimental data (e.g. cytokine concentrations and immune cell counts) measured in pony lungs infected with H3N8 virus, while the Hancioglu model was fit to certain qualitative behaviors selected from a study of the human response to IAV infection by Bocharov and Romanyukha [22].

Five elements of the intrahost immune response are conserved across each model: healthy epithelial cells (H), infected cells (I), virus (V), type I interferon (F), and "resistant cells", i.e. epithelial cells with interferon-induced virus resistance (R). While each model has these five features in common, the inflammatory response to viral infection is represented differently, depending largely on model complexity. These differences are particularly apparent in the model-specific incorporation of the production, activity, and depletion of IFN. In the Pawelek model (Figure 1a), interferon has two functions: creating virus-resistant cells when interacting with healthy epithelial cells, and increasing infected cell death when interacting with infected epithelial cells. In the Saenz model (Figure 1b), interferon leads to the creation of virus-resistant cells but does not impact the infected cells directly. Instead, the infected cells produce more interferon. The Hancioglu model (Figure 1c) uses interferon to create resistant cells (as in the other two models) while interferon is produced by

infected cells and antigen-presenting cells. In all models, a decrease in interferon levels is caused by a combination of natural decay and absorption into epithelial cells.

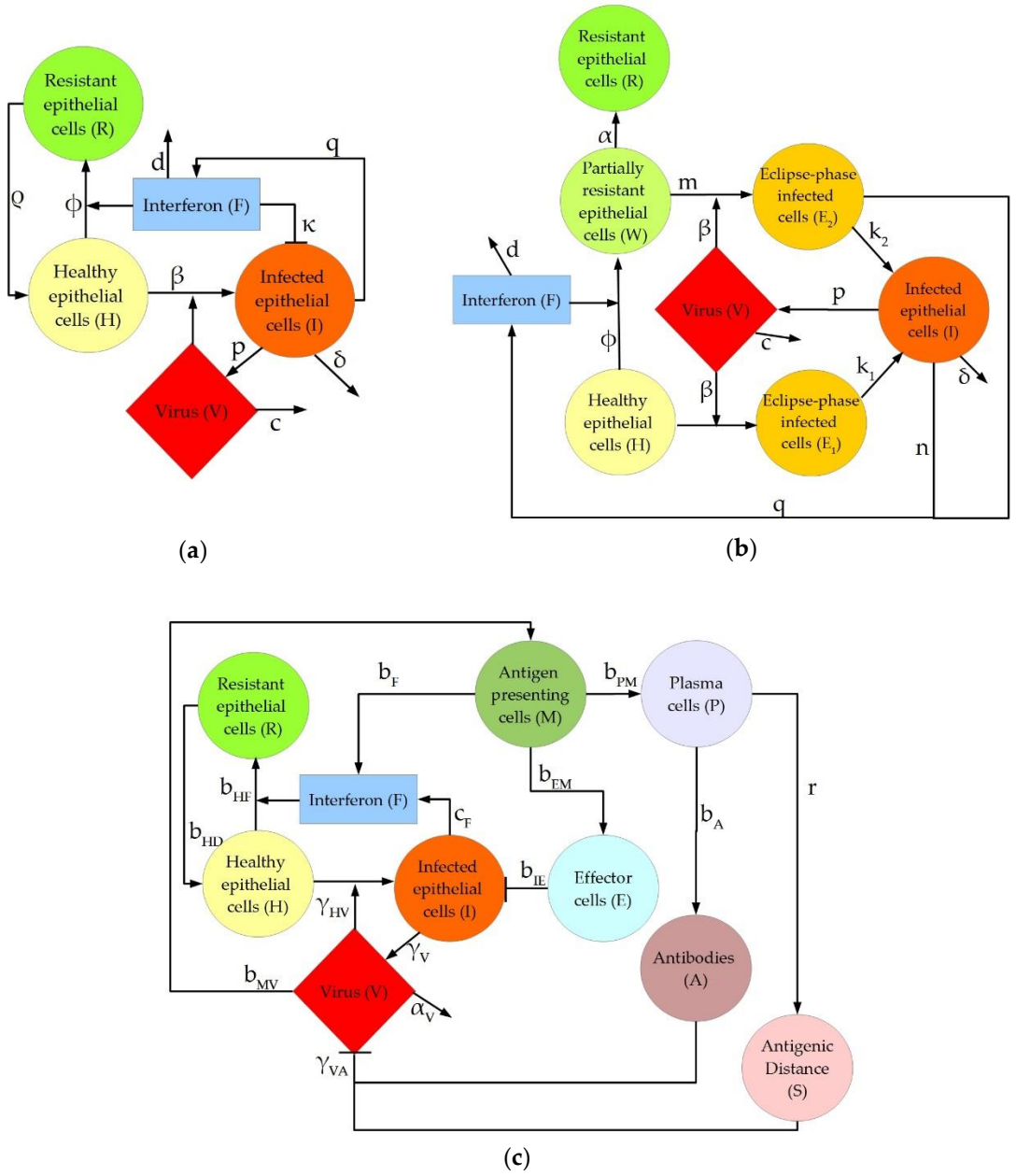

Figure 1. Graphical depiction of interactions represented in the three models discussed in this manuscript: (**a**) Pawelek model; (**b**) Saenz model; (**c**) Hancioglu model.

2. Materials and Methods

Three ordinary differential equation (ODE) models of the intrahost immune response to IAV infection that explicitly included type I interferon were chosen from literature. These three published models were selected for their significant variance in complexity; specifically, in the interactions of IFN with other model components. For each model, the immune response is simulated in MATLAB version R2017a using the parameter values and initial conditions published in the original papers. Integration was performed with ode23s.

We performed two main assessments on the three featured models: a local sensitivity analysis and an interferon pre-treatment study. Sensitivity analysis was performed using a MATLAB package

previously published by Nagaraja et al [23]. The Param_var_local.m function performed a local sensitivity analysis on the virus equation in each model to all parameters over a ten day simulation. This sensitivity analysis was additionally used in the calculation of area under the curve (AUC) for each parameter. Parameters which yield the highest AUC over the full ten day simulation are judged to be the most sensitive.

Two tests were used to evaluate each model's reaction to simulated interferon treatments. First, five values of the initial level of the IFN present in the system (F0) were tested to assess whether increased initial IFN levels will inhibit viral growth, peak, or clearance. In each case, while the initial condition on the IFN equation changed, all other initial conditions and parameters remain constant. Additionally, the amount of time between the initial IFN administration and the start of the infection was varied by delaying the onset of the virus with respect to the IFN. The 6 possible delays in the virus administration included 0, 2, 4, 6, 8, and 10 days (equivalent to pretreating with IFN 0, 2, 4, 6, 8, and 10 days prior to infection). The initial level of IFN is kept at 1 in these simulations, though the published initial condition of the fold change of IFN in the Saenz model is 0. To simulate a true pre-treatment, there must be a nonzero initial level of IFN to observe the impact of IFN on the remainder of the system.

3. Results

3.1. Sensitivity analysis

3.1.1. Pawelek et al. model

The Pawelek model includes five equations and nine parameters to model the intrahost immune response to IAV infection. Epithelial cells begin as healthy target cells (H) and can become infected (I) through direct interaction with the virus (V) or can become resistant to infection (R) through interaction with type I interferon (F). Interferon can also lead to enhanced infected cell clearance by stimulating the activation of natural killer cells, which are not explicitly represented in the model. The structure of the Pawelek model is given below in equations 3.1.1:

$$\begin{aligned} H' &= -\beta HV - \phi HF + \rho F, \\ I' &= \beta HV - \delta I, \\ R' &= \phi HF - \rho F, \\ V' &= pI - cV, \\ F' &= qI - dF. \end{aligned} \tag{3.1.1}$$

First, a local sensitivity analysis was used to identify model parameters to which the virus titer is most sensitive. The parameters which most affect the virus level change over time, as shown in Figure 2a. Over the first two days, the decay rate of interferon (d) and the production of resistant cells (ϕ) dominate the behavior of the virus. In the later phase of infection, virus behavior is controlled predominantly by the rate at which cells lose their resistance (ϱ), the death of infected cells (δ), and the depletion of interferon (d). This implies that in all stages of infection, virus levels are largely impacted by interferon and resistant cell populations. Given that interferon controls the number of resistant cells in the system, and thus the number of cells available to become infected by the virus, the production and depletion of interferon is expected to be vital to the control of the virus growth throughout the simulation. Over ten days, the parameters with the highest total AUC are the rate of loss of resistance in the epithelial cells (ϱ) and the decay rate of infected cells (δ).

Figure 2b depicts the model response to changing these two most sensitive parameters concurrently. Colors on the graph correspond to the amount of virus present in the system after ten days, where darker colors indicate more virus present. As δ increases, the infected cells die at a faster rate, and the virus cannot be sustained, leading to a lower virus level at the end of the ten day

simulation. As ϱ increases, the healthy epithelial cells regenerate at a faster rate, providing a larger pool of cells which may transition to infected cells and produce virus. Thus, as ϱ increases, more virus is expected to be present at the end of the simulation. However, the current formulation of the model may overfit the parameters, leading to unexpected trends in the end behavior of the virus. Specifically, similar values of ϱ and δ result in highly different responses. As more cells become resistant, there is greater feedback to the healthy cell population, allowing for a slight rebound in the target cell population. With more target cells available to become infected, there is an increase in virus over time. The structure of the model thus results in the creation of virus over time with the addition of more cells that are resistant to infection. This is an oversimplification of the interaction of interferon with epithelial cells, and is likely not a true representation of intrahost dynamics.

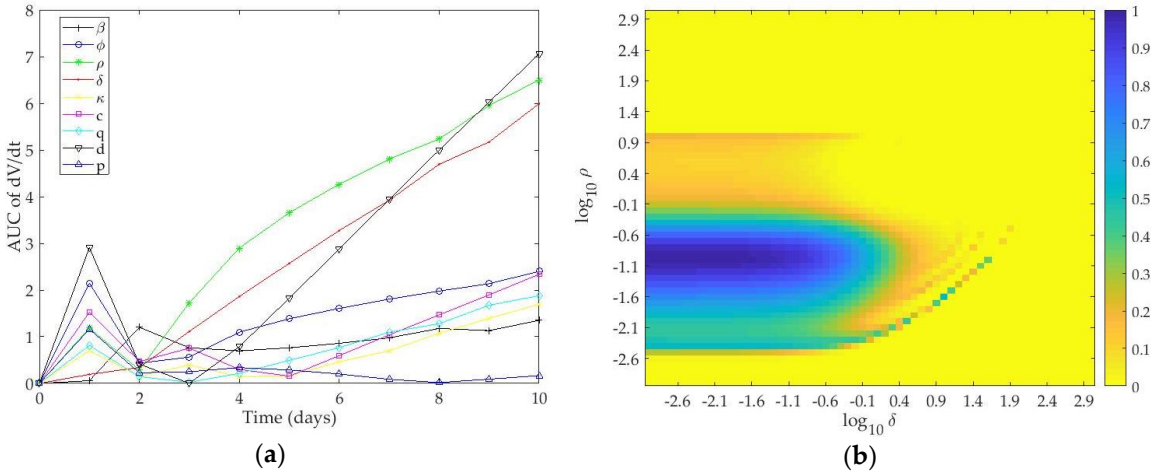

(**a**) (**b**)

Figure 2. (**a**) Time-dependent sensitivity of virus to each parameter in the Pawelek model; (**b**) Two-dimensional sensitivity of Pawelek model to two most sensitive parameters: ϱ and δ. Colors correspond to the amount of virus present at ten days post-infection in simulation. Darker blue colors correspond to a higher level of virus present, while more yellow colors indicate a low level of virus present in the system after ten days.

3.1.2. Saenz et al. model

The Saenz model includes eight equations and twelve parameters. The epithelial cell population is divided into six subtypes, based on whether these cells have been infected with virus (V) and/or affected by type I interferon (F). Cells can be healthy cells (H), infected cells that are unprotected by interferon (E1), partially resistant healthy cells (W), infected cells that have been affected by interferon (E2), productively infected cells (I), or fully resistant cells (R). The structure of the Saenz model is given below in equations 3.1.2:

$$
\begin{aligned}
H' &= -\beta HV - \phi HF, \\
E_1' &= \beta HV - k_1 E_1, \\
W' &= \phi FH - m\beta VW - \alpha W, \\
E_{2'} &= m\beta VW - k_2 E_2, \\
R' &= \alpha W, \\
I' &= k_1 E_1 + k_2 E_2 - \delta I, \\
V' &= pI - cV, \\
F' &= nqE_2 - dF + qI.
\end{aligned}
\tag{3.1.2}
$$

We explored the time-dependent sensitivity of the virus to each parameter in the model (Figure 3a). The first three days post-infection are predominantly controlled by the infectivity of the virus (β), production of virus by infected cells (p), and creation of unprotected infected cells (k_1). The later phase of the infection is controlled by death of infected cells (δ) and the eclipse phase period of interferon-protected infected cells (k_2). As in the Pawelek model, controlling the death rate of infected cells indirectly controls the death rate of the virus, as infected cells are the only source of free virus in the system. The eclipse phase also indirectly controls the virus production, since infected cells begin producing free virus as soon as the eclipse phase ends and become productively infected cells. The parameters most closely related to IFN concentration in the model (n, q, d, and ϕ) are not among the most sensitive for the virus in this model.

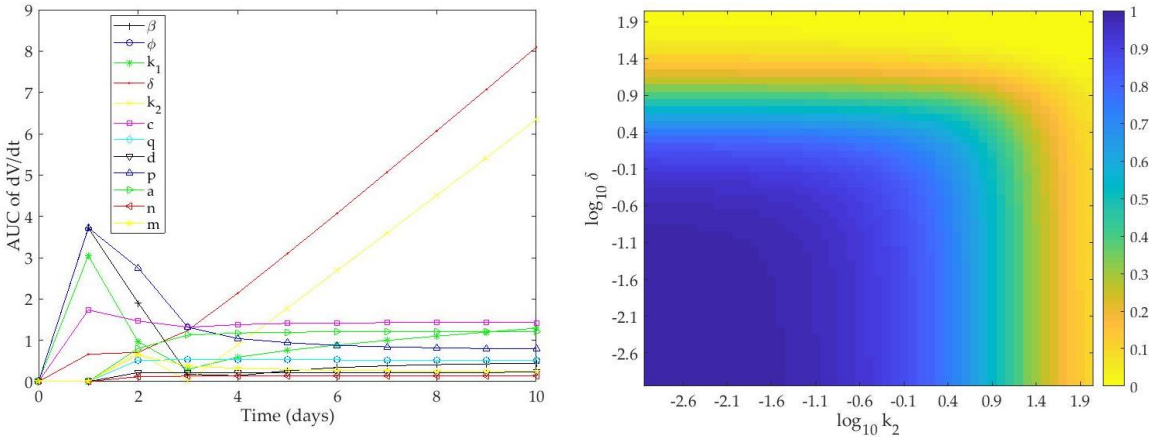

(**a**) (**b**)

Figure 3. (**a**) Time-dependent sensitivity of virus to each parameter in the Saenz model; (**b**) Two-dimensional sensitivity of Saenz model to two most sensitive parameters: k_2 and δ. Colors correspond to the amount of virus present at ten days post-infection in simulation. Darker blue colors correspond to a higher level of virus present, while more yellow colors indicate a low level of virus present in the system after ten days.

A two-dimensional scan of the most sensitive parameters to the clearance rate of the virus from the host is shown in Figure 3b. As expected, when k_2 and δ are high, the infected cells die at an increased rate and the virus is completely cleared from the host after ten days. When these parameters are low, however, the infected cell population is sustained and the virus is remains at high levels ten days post-infection.

3.1.3. Hancioglu et al. model

The Hancioglu model is the largest and most complex of the three models, featuring ten equations and 29 parameters. The model includes healthy (H), resistant (R), and infected (I) epithelial cells, virus (V), and interferon (F), as in the previous models. In addition, macrophages, T cells, plasma cells, antibodies, and antigenic distance are incorporated, as shown in Figure 1c. The equations which define the Hancioglu model are given below in (3.1.3):

$$H' = b_{HD}D(H+R) + a_R R - \gamma_{HV} VH - b_{HF} FH,$$

$$I' = \gamma_{HV} VH - a_I I - b_{IE} EI,$$

$$R' = b_{HF} FH - a_R R,$$

$$V' = \gamma_V I - \gamma_{VA} SAV - \gamma_{VH} HV - \alpha_V V - \frac{a_{v1} V}{a_{v2} V + 1}, \quad (3.1.3)$$

$$M' = (1-M)(b_{MD}D + b_{MV}V) - a_M M,$$

$$F' = b_F M + c_F I - b_{FH} HF - a_F F,$$

$$E' = b_{EM} ME - b_{EI} IE + a_E(1-E),$$

$$P' = b_{PM} MP + a_P(1-P),$$

$$A' = b_A P - \gamma_{AV} SAV - a_A A,$$

$$S' = rP(1-S).$$

Figure 4a shows the sensitivity of the virus equation to each of the parameters of the model. The early stage infection is largely controlled by virus production by infected cells (γ_V), infected cell death (a_I), and loss of resistance in epithelial cells (a_R). All three of these parameters are essential to controlling the infected cell population, which, like in the previous two models, controls the amount of free virus produced by the host. In the later stages of infection, the decay rate of IFN (a_F) and the infectivity of the virus (γ_{VH}) become most influential on the virus trajectory.

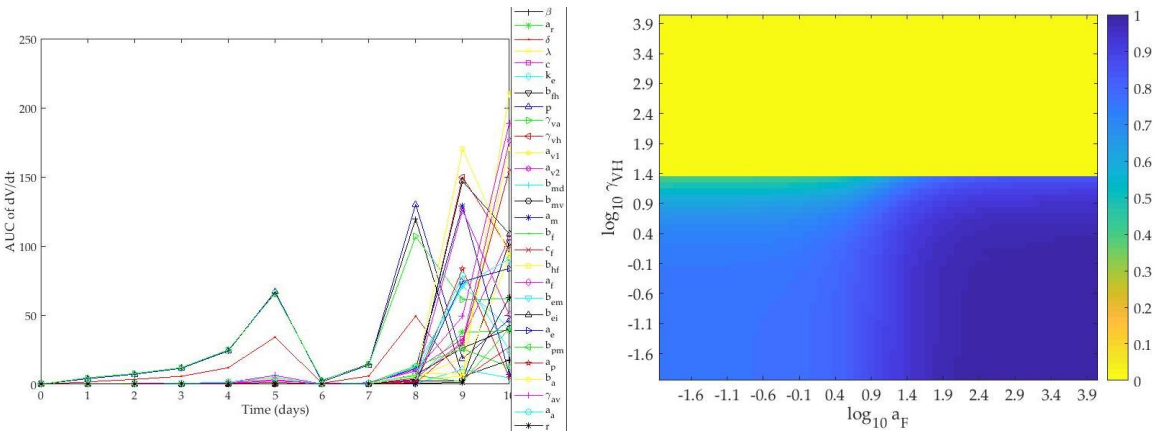

(**a**) (**b**)

Figure 4. (**a**) Time-dependent sensitivity of virus to each parameter in the Hancioglu model; (**b**) Two-dimensional sensitivity of Hancioglu model to two most sensitive parameters: γ_{VH} and a_F. Colors correspond to the amount of virus present at ten days post-infection in simulation. Darker blue colors correspond to a higher level of virus present, while more yellow colors indicate a low level of virus present in the system after ten days.

The amount of virus present at the end of the simulation changes dramatically based on the initial level of γ_{VH} used in the simulation, as shown in Figure 4b. Varying γ_{VH} causes a bifurcation in virus behavior, where high levels cause a monotonic decay in the virus from day 0 to the end of the simulation. Below $\log_{10}(\gamma_{VH}) = 1.4$, the virus can reach a peak level of around 100 (approximately four orders of magnitude greater than the initial level of virus present on day 0). Then, depending on the value of a_F, the presence of interferon can be sufficient for the virus to decay to zero by the end of the simulation (low a_F values) or the virus will remain high for over two weeks post-infection (high a_F values).

3.2. Models' response to simulated IFN pre-treatment

We simulated IFN pre-treatment in these models by changing the time and magnitude of the initial interferon levels in the system. Though some recommendations say that interferon should be administered at least ten days pre-infection [10], there is no clear consensus on exactly how early or with what magnitude the IFN should be administered to the patient. For each model, the response to changing both the magnitude of the initial interferon levels and the time between the initial interferon injection and the viral infection is reported.

3.2.1 Pawelek model response to IFN stimulation

Figure 5a depicts the impact of altering the initial levels of IFN (F0) present in the system when the virus is administered. The Pawelek model predicts three phases of behavior based on the amount of interferon initially administered to the host. At high levels of interferon, there is a quick rise in the virus followed by a slow decay, leading to eventual clearance from the host. When F0 is 1, the virus exhibits biphasic behavior, with an initial peak approximately 12 hours post-infection and a second peak around 2 days post-infection, followed by slow clearance of the virus over the next week. When F0 is very low (less than 1), the same initial peak after 12 hours is followed by a long, slow rise in the virus trajectory after day 3. At high levels of F0, the virus peak is about 2 orders of magnitude lower than the other simulations, and the healthy cells show a slight rebound before dying out around 1 day post-infection. The IFN also monotonically decays when it is initially set to a high level and does not show the same rebound behavior seen in lower initial levels of IFN. Despite these three differences, it is difficult to determine how these rebounding virus trajectories would impact the survival of the host. The Pawelek model leads to complete death of all healthy cells in all trajectories, meaning there are no target cells remaining for the virus to infect after a few days of the infection. Because of this, the Pawelek model cannot accurately predict whether high initial doses of IFN would save the host.

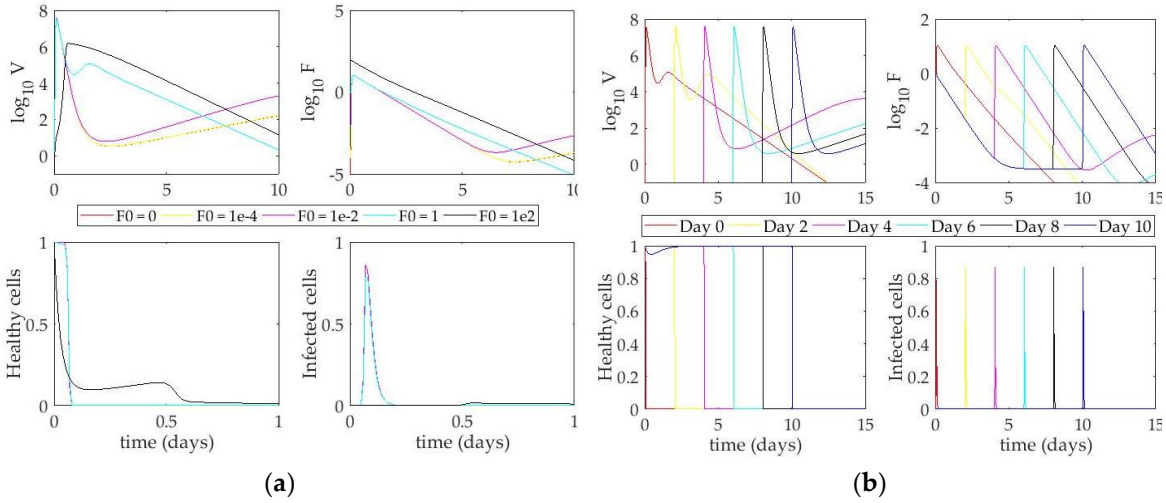

Figure 5. (**a**) Response of Pawelek model to increasing IFN on day 0. Lines correspond to different values of F0 (initial condition of interferon); (**b**) Impact of IFN pre-treatment scheduling on the Pawelek model. IFN treatment is given on day 0 and patients are simulated to become infected 2, 4, 6, 8, or 10 days after treatment.

The impact of changing the time between the IFN pre-treatment and the onset of the infection is shown in Figure 5b. Each line denotes a different simulation in which the virus is administered at the indicated day on the figure legend. Again, changing the time between treatment and infection causes three phases of behavior in the virus. When IFN and virus are given simultaneously (red "Day 0" line), the simulation describes the behavior of an untreated patient. In this case, the virus peaks almost immediately, falls, and then exhibits a smaller, secondary peak around day 2 as the infected cells have time to produce more virus.

The other simulations in Figure 5b show that the Pawelek model predicts a negative impact on the host after IFN pre-treatment. With a 2-day pre-treatment (yellow line), the virus trajectory is approximately the same as the nominal model. The initial peak reaches the same magnitude as the nominal model, but the secondary peak is more pronounced. When IFN is given before the virus, there are no infected cells present in the system (which are the only sources of IFN in this model). Thus, the IFN levels will decrease until the virus is introduced on day 2. At that point, the IFN has decreased approximately two orders of magnitude, meaning the initial treatment was not sustained and has had a deleterious effect on the host, as there is less IFN present in the system than under normal circumstances.

As the delay between IFN and virus lengthens, this effect becomes more pronounced. While the initial virus peak always reaches the same magnitude, the secondary peak, which controls the long-term behavior of the system, gets larger with the increased delay. This indicates that the model predicts a chronic influenza infection after significant IFN pre-treatment rather than any improvement in patient outcomes, regardless of the length of time between virus and IFN treatment.

3.2.2 Saenz model response to IFN treatment

The response of the Saenz model to an increase in the initial IFN present in the system is shown in Figure 6a. Changing the level of IFN creates a bifurcation in the virus peak magnitude. When F0 is below 1, the virus peak reaches 10^5 PFU (a 5-fold change in the virus level). IFN and infected cells rise to their peaks around 3 days post-infection, and healthy cells die out within 2 days. When F0 is above 1, however, the virus peak only reaches approximately 10 PFU. IFN decays monotonically, and almost no infected cells are created. Healthy cells die out almost instantly upon infection, as more resistant cells can be created from the increased initial IFN levels.

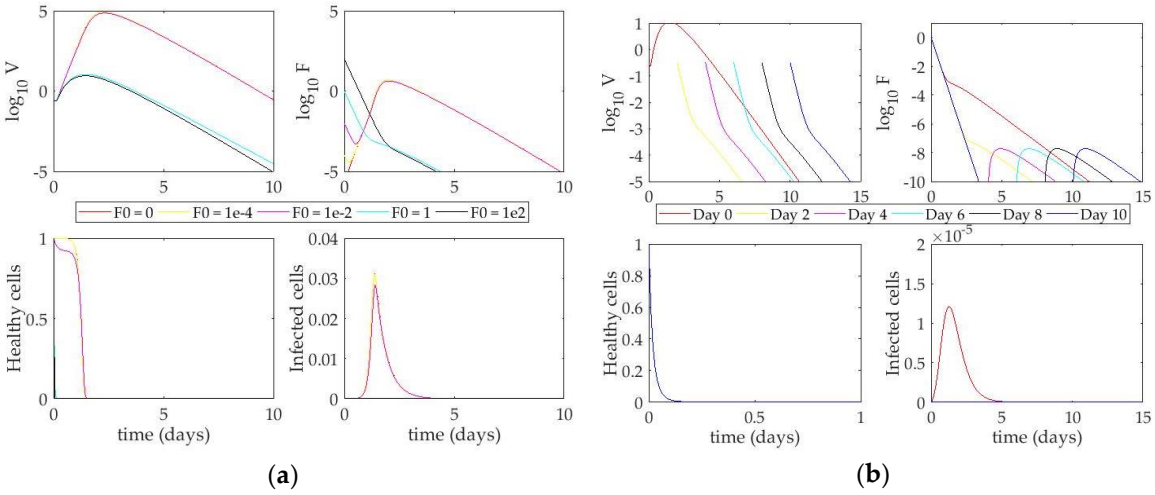

Figure 6. (**a**) Response of Saenz model to increasing IFN on day 0. Lines correspond to different values of F0 (initial condition of interferon); (**b**) Impact of IFN pre-treatment scheduling on the Saenz model. IFN treatment is given on day 0 and patients are simulated to become infected 2, 4, 6, 8, or 10 days after treatment.

Figure 6b illustrates the impact of IFN pre-treatment on the system. The nominal model (red "Day 0" line) is equivalent to the turquoise line (F0=1) in Figure 6a. As the time between the initial IFN and virus increases, we see the pre-treatment confers protection on the host by creating a larger pool of resistant cells initially, leading to a depletion of healthy cells within hours of the initiation of the simulation. When the host becomes infected, there is not a large enough pool of healthy cells available to create any substantial infected cell population. Without these cells, no new virus can be produced, so the virus monotonically decays to zero within only a few days post-infection.

Like the Pawelek model, the Saenz model cannot support high levels of IFN without the presence of virus, as only infected cells can produce more IFN. In all simulations, the IFN decays steadily and more rapidly than in the Pawelek simulations in Figure 5. This is largely due to the differences in the decay rate of IFN between the two models (Pawelek model, d = 1.9 day^{-1}, Saenz model, d = 6.8 day^{-1}).

3.2.3 Hancioglu model response to IFN treatment

The Hancioglu model (Figure 7) shows very little sensitivity to the time of IFN administration or the magnitude of interferon. There is a negligible difference in the time to the peak of the virus when F0 = 1 versus F0 = 100. The model's parameters were fit in a way such that the behavior of the model does not change, even with an enormous initial influx of interferon. An initial absence of

interferon has no impact on the virus trajectory. Despite the presence of resistant cells in the model, interferon has no major effect on the system.

When the system is tested with a pre-treatment of interferon (Figure 7b), there is little change in the behavior of the virus. The entire system shifts horizontally with the time delay, but the overall behavior of the model does not change. Like in previous models, without a starting virus population, the system cannot sustain the initial concentration of IFN. When the virus is finally introduced, the IFN level has essentially fallen to zero, making any impact from the pre-treatment negligible.

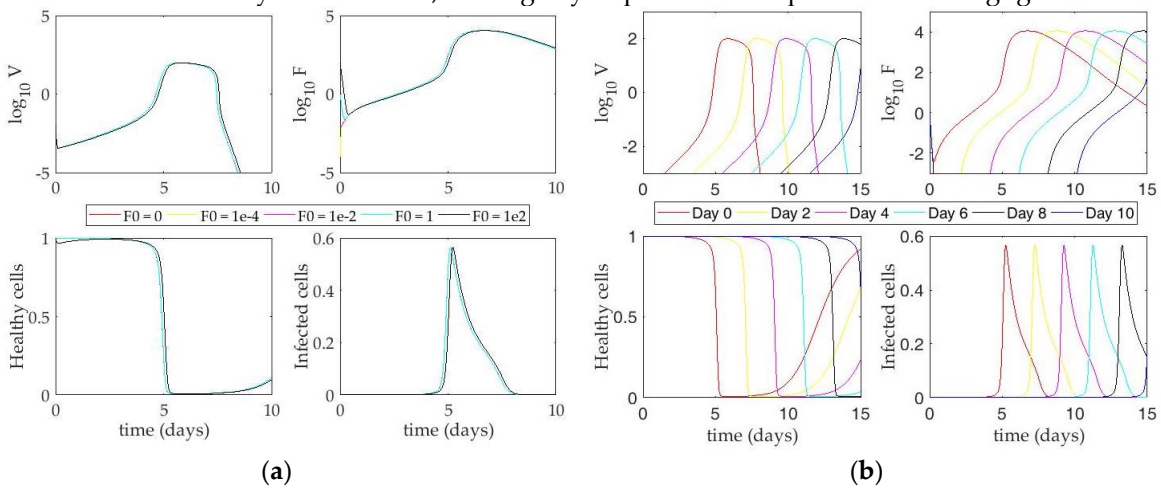

Figure 7. (**a**) Response of Hancioglu model to increasing IFN on day 0. Lines correspond to different values of F0 (initial condition of interferon); (**b**) Impact of IFN pre-treatment scheduling on the Hancioglu model. IFN treatment is given on day 0 and patients are simulated to become infected 2, 4, 6, 8, or 10 days after treatment.

4. Discussion

Interferon is known to have several antiviral effects in an IAV-infected host, including activating an antiviral state in epithelial cells, sensitizing cells to apoptosis, activating NK cells, and initiating the differentiation of cytotoxic T cells [24–27]. Each analyzed model represents a distinct subset of these interactions, including the creation and depletion of virus-resistant cells. In the Pawelek model, IFN is only produced by infected cells, and healthy cells can become resistant through an interaction with IFN. This resistance fades over time and cells return to a susceptible state. Resistant cells in the Hancioglu model also become susceptible, but IFN can be produced by either infected cells or antigen presenting cells. Conversely, the Saenz model features epithelial cells that are either partially or fully resistant to infection, and cells do not lose resistance over time.

All models must make some simplifying assumptions, and thus, no models are fully accurate in their representation of the host response to IFN treatment. While these models had been analyzed in previous reviews [28], previous work had only shown how these models respond to knockouts of various immune components. Here, we perform a complementary study to test early administration as well as increased initial levels of IFN to determine if altering IFN levels can improve patient outcomes. Of the three models studied, only one showed significant impact after early IFN treatment. The Saenz model predicts a lower viral peak with increased initial interferon levels and a monotonic decay of the virus over time if interferon is administered early. Early available interferon creates a large pool of resistant cells in a short period of time and, because the Saenz model does not allow for loss of resistance in cells over time, resistant cells remain resistant for the rest of the simulation. Thus, the system cannot replenish the source of target cells for the virus to infect and the virus concentration decreases steadily. However, this is not a realistic way to represent immune dynamics, as epithelial cells certainly lose their viral resistance over time.

The other two models do not demonstrate this effect of IFN on viral clearance. The Pawelek model is structured such that early administration of interferon worsens the impact of the virus by creating a secondary rebound of virus in later stages of infection, essentially leading to chronic

infection (which is unlikely to be realistic). The Hancioglu model shows no sensitivity to the initial interferon level or to the timing of infection. Changing the time of the virus administration simply shifts the curves in time but does not change their shape. This model implies that interferon has minimal impact on the host, which does not agree with most experimental results [29,30].

By stimulating an early IFN response in the model, we simulate a host receiving a preventative treatment for IAV infection. Dobrovolny et al [28] previously investigated how these models react to IFN suppression, which may suffice to simulate a steroid treatment for influenza as steroids are known to downregulate IFN signaling [10,31]. The Hancioglu and Pawelek models predict that IFN has a significant impact on viral clearance when completely removed from the system because no resistant cells are created and the population of susceptible cells remains high for a longer period of time [28]. In the Saenz model, however, removing IFN does not yield this effect, as cells in this model cannot lose resistance. Therefore, these models may not accurately represent the effect of IFN pre-treatment for influenza, as they make many simplifying assumptions about the role of IFN in the host immune response to IAV infection.

Currently, we do not have sufficient experimental or computational evidence to support a recommendation for IFN pretreatment or corticosteroid treatment post-infection. Few references exist showing steroid treatment of IAV-infected humans [9,32–34], and those few have not shown significant impacts on mortality rate [35]. For many years, physicians turned toward high doses of steroids, though recent research suggests that lower doses are more effective [35,36]. It is quite possible that steroid treatment could be effective in humans, but the timing and magnitude of the drug has not yet been optimized. Some reports suggest that the treatment should be given at least ten days pre-infection [10], which is likely not practical for the average person. It is also suggested that steroid therapy should be combined with oseltamivir treatment [10,37], but given the disparate effects of early and diminished IFN in the mathematical models, we cannot simulate the effectiveness of this approach.

While the models presented do capture many aspects of the immune response to IAV infection, we cannot be certain that IFN pre-treatment is accurately portrayed in these models without more experimental data with which to train the models. An experiment in which hosts are treated with interferon days before the virus is administered is vital for validating the models' behavior. These experiments will also inform future treatment plans for appropriate timing and magnitude of IFN administration in virus-infected hosts.

Acknowledgments: The authors acknowledge funding support from the University of Pittsburgh's Swanson School of Engineering.

Author Contributions: E.M. and J.E.S. conceived and designed the experiments; E.M. performed the experiments; E.M., E.A., and J.E.S. analyzed the data; E.M., E.A., and J.E.S. wrote the paper.

Conflicts of Interest: The authors declare no conflict of interest. The founding sponsors had no role in the design of the study; in the collection, analyses, or interpretation of data; in the writing of the manuscript, and in the decision to publish the results.

References

1. World Health Organization Influenza (Seasonal).
2. Potter, C. W. A history of influenza. *J. Appl. Microbiol.* **2001**, *91*, 572–579, doi:10.1046/j.1365-2672.2001.01492.x.
3. Kilbourne, E. D. Influenza pandemics of the 20th century. *Emerg. Infect. Dis.* **2006**, *12*, 9–14, doi:10.3201/eid1201.051254.
4. James R. Gill , MD, Zong-Mei Sheng , MD, PhD, Susan F. Ely , MD, MPHTM, Donald G. Guinee Jr , MD, Mary B. Beasley , MD, James Suh , MD, Charuhas Deshpande , MD, Daniel J. Mollura , MD, David M. Morens , MD, Mike Bray , MD, William D. Travis , MD, and Jeff, P. Pulmonary Pathologic Findings of Fatal 2009 Pandemic Influenza A/H1N1 Viral Infections. *Arch. Pathol. Lab. Med.* **2010**, *134*.
5. Chotpitayasunondh, T.; Ungchusak, K.; Hanshaoworakul, W.; Chunsuthiwat, S.; Sawanpanyalert, P.; Kijphati, R.; Lochindarat, S.; Srisan, P.; Suwan, P.; Osotthanakorn, Y.; Anantasetagoon, T.; Kanjanawasri, S.; Tanupattarachai, S.; Weerakul, J.; Chaiwirattana, R.; Maneerattanaporn, M.; Poolsavatkitikool, R.; Chokephaibulkit, K.; Apisarnthanarak, A.; Dowell, S. F. Human disease from influenza A (H5N1), Thailand, 2004. *Emerg. Infect. Dis.* **2005**, *11*, 201–209, doi:10.3201/eid1102.041061.
6. Truong, N. T.; Long, H. T.; Ph, D.; Tung, C. V.; Giang, L. T.; Ph, D. Avian influenza A (H5N1) in 10 patients in Vietnam. *N. Engl. J. Med.* **2004**, *350*, 1179–1188.
7. Liu, Q.; Zhou, Y. H.; Yang, Z. Q. The cytokine storm of severe influenza and development of immunomodulatory therapy. *Cell. Mol. Immunol.* **2016**, *13*, 3–10, doi:10.1038/cmi.2015.74.
8. Hayden, F. G. Antiviral Resistance in Influenza Viruses — Implications for Management and Pandemic Response. *N. Engl. J. Med.* **2006**, *354*, 785–788.
9. Beigel, J. H.; Farrar, J.; Han, A. M.; Hayden, F. G.; Hyer, R.; de Jong, M. D.; Lochindarat, S.; Tien, N. T. K.; Hein, N. T. Avian influenza A (H5N1) infection in humans. *N Engl J Med* **2005**, *353*, 1374–1385.
10. Carter, M. J. A rationale for using steroids in the treatment of severe cases of H5N1 avian influenza. *J. Med. Microbiol.* **2007**, *56*, 875–883, doi:10.1099/jmm.0.47124-0.
11. Shinya, K.; Ito, M.; Makino, A.; Tanaka, M.; Miyake, K.; Eisfeld, A. J.; Kawaoka, Y. The TLR4-TRIF Pathway Protects against H5N1 Influenza Virus Infection. *J. Virol.* **2012**, *86*, 19–24, doi:10.1128/JVI.06168-11.
12. Kudo, K.; Takasaki, J.; Manabe, T.; Uryu, H.; Yamada, R.; Kuroda, E.; Kobayashi, N.; Matsushita, T. Systemic corticosteroids and early administration of antiviral agents for pneumonia with acute wheezing due to influenza a(h1n1)pdm09 in japan. *PLoS One* **2012**, *7*, doi:10.1371/journal.pone.0032280.
13. Brun-Buisson, C.; Richard, J.-C. M.; Mercat, A.; Thiébaut, A. C. M.; Brochard, L. Early Corticosteroids in Severe Influenza A/H1N1 Pneumonia and Acute Respiratory Distress Syndrome. *Am. J. Respir. Crit. Care Med.* **2011**, *183*, 1200–1206, doi:10.1164/rccm.201101-0135OC.
14. Ottolini, M.; Blanco, J.; Porter, D.; Peterson, L.; Curtis, S.; Prince, G. Combination of anti-inflammatory and antiviral therapy of influenza in a cotton rat model. *Pediatr Pulmonol* **2003**, *36*, 290–294.
15. Pawelek, K. A.; Huynh, G. T.; Quinlivan, M.; Cullinane, A.; Rong, L.; Perelson, A. S. Modeling within-host dynamics of influenza virus infection including immune responses. *PLoS Comput. Biol.* **2012**, *8*, e1002588, doi:10.1371/journal.pcbi.1002588.
16. Saenz, R. A.; Quinlivan, M.; Elton, D.; Macrae, S.; Blunden, A. S.; Mumford, J. A.; Daly, J. M.; Digard, P.; Cullinane, A.; Grenfell, B. T.; McCauley, J. W.; Wood, J. L. N.; Gog, J. R. Dynamics of influenza virus infection and pathology. *J. Virol.* **2010**, *84*, 3974–83, doi:10.1128/JVI.02078-09.
17. Hancioglu, B.; Swigon, D.; Clermont, G. A dynamical model of human immune response to influenza A

virus infection. *J. Theor. Biol.* **2007**, *246*, 70–86, doi:10.1016/j.jtbi.2006.12.015.

18. Baccam, P.; Beauchemin, C.; Macken, C. a; Hayden, F. G.; Perelson, A. S. Kinetics of influenza A virus infection in humans. *J. Virol.* **2006**, *80*, 7590–9, doi:10.1128/JVI.01623-05.
19. Handel, A.; Longini, I. M.; Antia, R. Towards a quantitative understanding of the within-host dynamics of influenza A infections. *J. R. Soc. Interface* **2010**, *7*, 35–47, doi:10.1098/rsif.2009.0067.
20. Bocharov, G. a.; Romanyukha, a. a. Numerical treatment of the parameter identification problem for delay-differential systems arising in immune response modelling. *Appl. Numer. Math.* **1994**, *15*, 307–326, doi:10.1016/0168-9274(94)00007-7.
21. Price, I.; Mochan-Keef, E. D.; Swigon, D.; Ermentrout, G. B.; Lukens, S.; Toapanta, F. R.; Ross, T. M.; Clermont, G. The inflammatory response to influenza A virus (H1N1): An experimental and mathematical study. *J. Theor. Biol.* **2015**, *374*, 83–93, doi:10.1016/j.jtbi.2015.03.017.
22. Bocharov, G. A.; Romanyukha, A. A. Mathematical Model of Antiviral Immune Response III. Influenza A Virus Infection. *J Theor Biol* **1994**, *167*, 323–360.
23. Nagaraja, S.; Wallqvist, A.; Reifman, J.; Mitrophanov, A. Y. Computational Approach To Characterize Causative Factors and Molecular Indicators of Chronic Wound Inflammation. *J. Immunol.* **2014**, *192*, 1824–1834, doi:10.4049/jimmunol.1302481.
24. Biron, C. a Role of early cytokines, including alpha and beta interferons (IFN-alpha/beta), in innate and adaptive immune responses to viral infections. *Semin. Immunol.* **1998**, *10*, 383–390, doi:10.1006/smim.1998.0138.
25. García-Sastre, A.; Durbin, R. K.; Zheng, H.; Palese, P.; Gertner, R.; Levy, D. E.; Durbin, J. E. The role of interferon in influenza virus tissue tropism. *J. Virol.* **1998**, *72*, 8550–8558.
26. Stark, G. R.; Kerr, I. M.; Williams, B. R.; Silverman, R. H.; Schreiber, R. D. How cells respond to interferons. *Annu. Rev. Biochem.* **1998**, *67*, 227–264.
27. van Boxel-Dezaire, A. H. H.; Rani, M. R. S.; Stark, G. R. Complex modulation of cell type-specific signaling in response to type I interferons. *Immunity* **2006**, *25*, 361–372.
28. Dobrovolny, H. M.; Reddy, M. B.; Kamal, M. a; Rayner, C. R.; Beauchemin, C. a a Assessing mathematical models of influenza infections using features of the immune response. *PLoS One* **2013**, *8*, e57088, doi:10.1371/journal.pone.0057088.
29. Fensterl, V.; Sen, G. C. Interferons and viral infections. *Biofactors* **2009**, *35*, 14–20, doi:10.1002/biof.6.
30. Pestka, S.; Krause, C. D.; Walter, M. R. Interferons, interferon-like cytokines, and their receptors. *Immunol. Rev.* **2004**, *202*, 8–32.
31. Flammer, J. R.; Dobrovolna, J.; Kennedy, M. A.; Chinenov, Y.; Glass, C. K.; Ivashkiv, L. B.; Rogatsky, I. The Type I Interferon Signaling Pathway Is a Target for Glucocorticoid Inhibition . *Mol. Cell. Biol.* **2010**, *30*, 4564–4574, doi:10.1128/MCB.00146-10.
32. Kandun, I. N.; Wibisono, H.; Sedyaningsih, E. R.; Yusharmen, D. P. H.; Hadisoedarsuno, W.; Purba, W.; Santoso, H.; Septiawati, C.; Tresnaningsih, E. Three Indonesian clusters of H5N1 virus infection in 2005. *N Engl J Med* **2006**, *355*, 2186–2194.
33. Yuen, K. Y.; Chan, P. K. S.; Peiris, M.; Tsang, D. N. C.; Que, T. L.; Shortridge, K. F.; Cheung, P. T.; To, W. K.; Ho, E. T. F. Clinical features and rapid viral diagnosis of huamn disease associated with avian influenza A H5N1 virus. *Lancet* **1998**, *351*, 467–471.
34. Hien, T. T.; Liem, N. T.; Dung, N. T.; San, L. T.; Mai, P. P.; Chau, N. van V.; Suu, P. T.; Dong, V. C.; Mai, L. T. Q.; Thi, N. T.; Khoa, D. B.; Phat, L. P.; Truong, N. T.; Long, H. T.; Tung, C. V.; Giang, L. T.; Tho, N. D.; Nga, L. H.; Tien, N. T. K.; San, L. H.; Tuan, L. Van; Dolecek, C.; Thanh, T. T.; de Jong, M.; Schultsz,

C.; Cheng, P.; Lim, W.; Horby, P.; Farrar, J.; World Health Organization International Avian Influenza Investigative Team Avian Influenza A (H5N1) in 10 Patients in Vietnam. *N. Engl. J. Med.* **2004**, *350*, 1179–1188, doi:10.1056/NEJMoa040419.

35. Bernard, G. The International Sepsis Forum's controversies in spesis: corticosteroids should not be routinely used to treat septic shock. *Crit Care* **2002**, *6*, 3884–386.

36. Annane, D.; Bellisant, E.; Bollaert, P. E.; Briegel, J.; Keh, D.; Kupfer, Y. Corticosteroids for severe sepsis and septic shock: a systematic review and meta-analysis. *BMJ* **2004**, *329*, 480.

37. Chotpitayasunondh, T.; Ungchusak, K.; Hanshaoworakul, W.; Chunsuthiwat, S.; Sawanpanyalert, P.; Kijphati, R.; Lochindarat, S.; Srisan, P.; Suwan, P.; Osotthanakorn, Y.; Anantasetagoon, T.; Kanjanawasri, S.; Tanupattarachai, S.; Weerakul, J.; Chaiwirattana, R.; Maneerattanaporn, M.; Poolsavathitikool, R.; Chokephaibulkit, K.; Apisarnthanarak, A.; Dowell, S. F. Human disease from influenza A (H5N1), Thailand, 2004. *Emerg. Infect. Dis.* **2005**, *11*, 201–9, doi:10.3201/eid1102.041061.

© 2018 by the authors. Submitted for possible open access publication under the terms and conditions of the Creative Commons Attribution (CC BY) license (http://creativecommons.org/licenses/by/4.0/).